Proceedings of the 9th U.S. National and 10th Canadian Conference on Earthquake Engineering
Compte Rendu de la 9ième Conférence Nationale Américaine et
10ième Conférence Canadienne de Génie Parasismique
July 25-29, 2010, Toronto, Ontario, Canada • Paper No 105

CYLIC PERFORMANCE OF SHEAR-CRITICAL REINFORCED CONCRETE BEAMS RETROFITTED WITH CARBON FRP

M. A. Colalillo[1] and S. A. Sheikh[2]

ABSTRACT

Ageing infrastructure and improved design code shear provisions has led to a situation in which many older structures are considered structurally deficient and are in need of repair or retrofit. These structures may be at risk of catastrophic failure if their shear-critical components fail in a brittle manner, which could be induced under a seismic event. An effective method for upgrading these shear-critical components is by applying externally bonded fibre reinforced polymers (FRP). Significant increases in reinforced concrete beam shear strength can be obtained with FRP, as shown by many experiments on relatively small beams subjected to static loading. An experimental program was undertaken with shear-critical large reinforced concrete beams tested under reversed cyclic loading, to simulate a seismic event. The beams were reinforced with varied amounts of transverse steel and various configurations of carbon FRP wraps. An objective of the experimental work was to determine the interaction between transverse steel and FRP, and the shear contributions of concrete, steel, and FRP. Additionally, the adequacy of provisions from various design codes was evaluated with respect to FRP strain limits and strength predictions.

Introduction

Research on the seismic performance of FRP-retrofitted reinforced concrete members has primarily focused on strengthening of columns and beam-column joints to promote a ductile collapse mechanism. However, limited work has been reported on shear-critical beams tested under reversed cyclic loading to simulate an earthquake (Anil 2006, Sakar 2009). Many existing reinforced concrete structures in seismic regions are inadequately designed for shear and at risk of catastrophic brittle failure during an earthquake. One such example is the cement pre-heater tower reported on by Duong (2007) that had shear-critical beams and was at risk of collapse in the event of an earthquake. Testing performed on a scaled-down frame of the tower at the University of Toronto showed that shear retrofit of the beams with FRP was effective at changing the system failure mode to flexure. Unfortunately, the test provided limited information concerning concrete and FRP shear contributions at failure as the beams no longer failed in shear.

[1]Ph.D. Candidate, Dept. of Civil Engineering, University of Toronto, Toronto, ON. M5S 1A4
[2]Professor, Dept. of Civil Engineering, University of Toronto, Toronto, ON. M5S 1A4

The primary goal of this research was to evaluate the performance of FRP retrofitted beams subject to reversed cyclic loading simulating a seismic event. Without consideration of FRP, the seismic design provisions of CSA A23.3-04 and ACI 318-08 suggest taking the shear capacity of concrete as zero in plastic hinging regions. On the contrary, from the limited available research (Duong 2007, Anil 2006) it appears that concrete is active in providing shear resistance up to FRP failure. Researchers (Bousselham 2006, Pellegrino 2002) have also shown the presence of internal transverse steel affects the shear resistance offered by FRP, which is not accounted for in the design codes. Thus, this research attempts to quantify the shear resisting contributions of concrete, transverse steel, and FRP. Since ACI 440.2R-08 and CSA S6-06 shear formulations for FRP-retrofitted beams were derived from the results of static testing, their validity under seismic loading is of importance.

Experimental Investigation

In this experimental program, fifteen reinforced concrete beams were tested in a three-point bending configuration under reversed cyclic loading. The specimens had the same geometry and longitudinal steel reinforcement, but different amounts of internal transverse steel. The beams were 650 mm deep by 400 mm wide, and were cast 3600 mm long (Fig. 1). Each beam was doubly reinforced in flexure with eight 30M (area = 700 mm^2) bars at both the top and bottom regions. The 30M bars had yield strength of 481 MPa and elastic modulus of 214 GPa. The longitudinal bars were placed in two layers resulting in an effective depth of 545 mm. The shear span measured between support and load point was 1675 mm, thus the shear span-depth ratio (*a/d*) was 3.07. The beams were cast in three batches, about three months prior to testing. At the time of testing, the concrete had cylinder compressive strengths between 47.5 MPa and 53.5 MPa, depending on the cast. The maximum aggregate size was 10 mm. The beams were cast with rounded edges having a radius of 38 mm, in accordance with CSA S6-06 requirements, to minimize stress concentrations in the FRP wrapped around the beam corners.

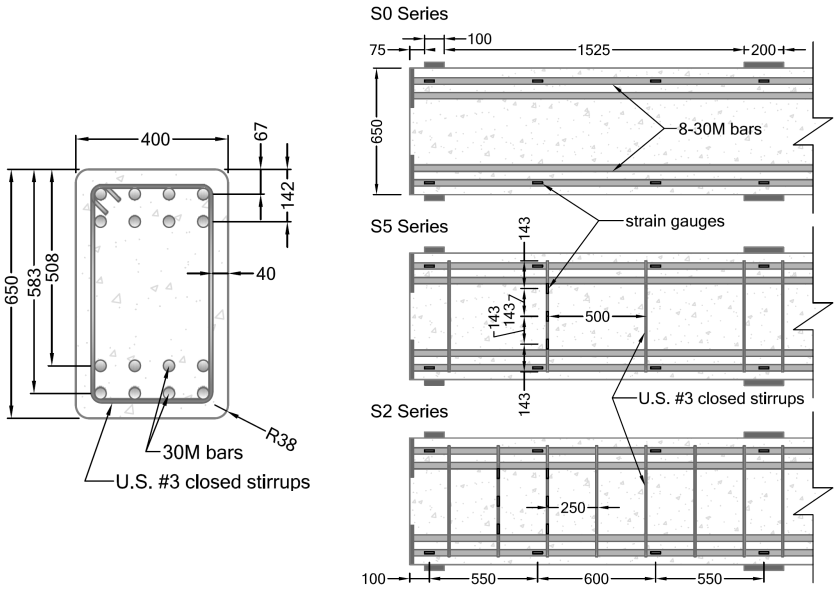

Figure 1. Steel reinforcement and instrumentation details.

Internal transverse steel consisted of U.S. #3 bars (area = 70.9 mm^2) formed into closed stirrups. The #3 bars had yield strength of 501 MPa and elastic modulus of 195 GPa. The specimens were divided into three series based on the amount of transverse steel used: S0 series having no transverse steel, S5 series with stirrups spaced at 500 mm, and S2 series with stirrups spaced at 250 mm. These spacing values were chosen to have beams with less (S5) and greater (S2) than the minimum amount of transverse steel recommended by CSA A23.3-04, CSA S6-06, and ACI 318-08. The S0 series specimens were intended as a benchmark against which contributions from transverse steel reinforcement could be evaluated.

Retrofit Details

Each series contained one un-retrofitted specimen as the control and four specimens that were shear retrofitted using externally bonded carbon FRP in the following configurations: U-wrapped strips (US), U-wrapped with continuous sheets (UA), closed wrapped strips (CS), and closed wrapped with continuous sheets (CA). The FRP composite system consisted of unidirectional carbon fibre fabric having a thickness of 1.0 mm. The composite had an ultimate tensile strain of 1.07% and an elastic modulus of 94.0 GPa. Retrofitting was done using a single layer with carbon fibres oriented transversely to the beam longitudinal axis. U-wraps were applied along the sides and bottom face of the beams, while closed wraps covered all four faces with a 100 mm overlap on the top face. The FRP strips were 100 mm wide and the centre-to-centre spacing was 200 mm (Fig. 2). For the U-wrapped strips, an additional 100 mm wide FRP strip was bonded longitudinally over the free strip ends to improve bond performance.

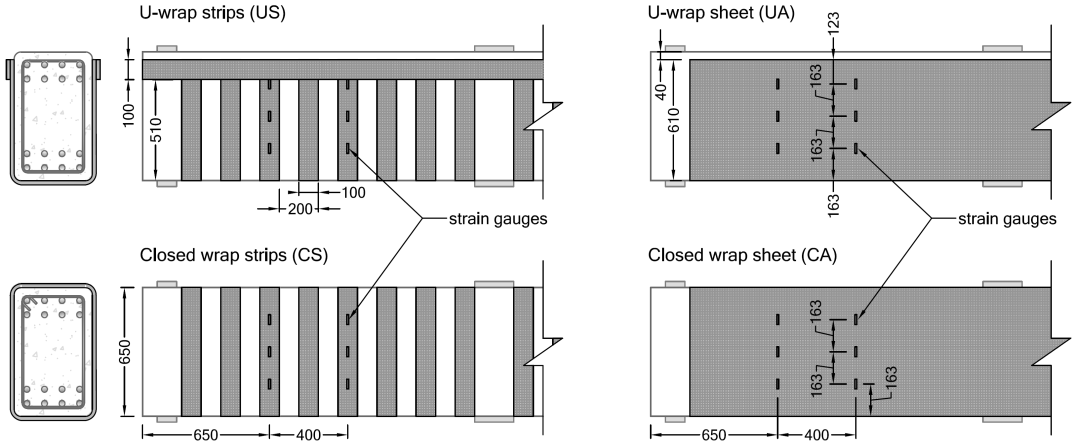

Figure 2. FRP retrofitting and instrumentation details.

Test Details

The specimens were tested in reversed cyclic loading under displacement control. A different cyclic loading scheme was used for each of the three beam series, as cycles were based on the failure load of the un-retrofitted controls. For each beam series, the control specimens were cycled twice at ±0.5 and ±0.75 times the approximate monotonic shear failure load predicted using CSA A23.3-04, after which point loading was continued in the downward direction until failure. The loading scheme of the retrofitted specimens consisted of two cycles at

each increasing interval of ±0.25 times the failure load of the control specimen for a particular series. Although shear failure was desired, specimens that reached flexural steel yielding were subjected to further cycles defined as increments of the yield displacement until FRP ruptured. The test setup is shown in Fig. 3. Roller bearings and plaster-filled bags were placed between the beams and the assembly supports, allowing for rotation and thereby providing a simple support condition. Shear failure was promoted in the more heavily instrumented span by applying three sets of steel clamps to the other span. Eleven linear variable displacement transducers (LVDT) were used to monitor deflections along the beam length and to determine shear strains. The longitudinal bars were strain gauged at five locations along the length of the beam (Fig 1). The S5 series specimens had two transverse steel stirrups instrumented with three strain gauges each, whereas S2 series specimens had four stirrups instrumented. Similarly, the FRP was strain gauged at four sections common to all specimens, with three gauges at each section (Fig. 2). The strain gauges were placed at three heights to obtain an average strain at the section.

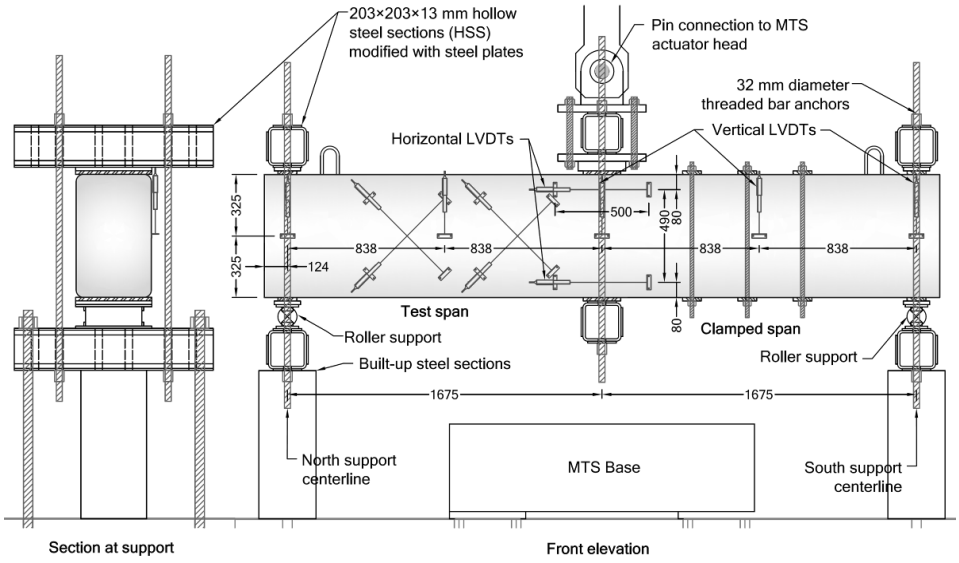

Figure 3. Test apparatus and LVDT layout.

Experimental Results

Shear force versus mid-span displacement curves are provided in Fig. 4, Fig. 5, and Fig 6 for the S0, S5, and S2 series, respectively. The failure shear and displacement values are also summarized in Table 1. As specimens had similar flexural properties, the onset of concrete cracking occurred at similar shears just over 100 kN. For the S0 control, the response slope was constant up to a shear of 226 kN after two reversals, followed by a sudden drop in load. With further loading, the peak shear reached was 275 kN. The two controls with transverse steel, S5 and S2, had similar response slopes to the S0 initial slope prior a shear of about 250 kN, corresponding to the formation of shear cracks and straining of the steel. These specimens failed in shear at 415 kN for S5 and 551 kN for S2. The FRP retrofitted specimen response curves were similar to those of their respective controls prior to the non-linear portion of the curve. With retrofitting, the curves remained relatively linear with increased load up to FRP failure, as the retrofitting limited crack width growth and thereby stiffened the beam response.

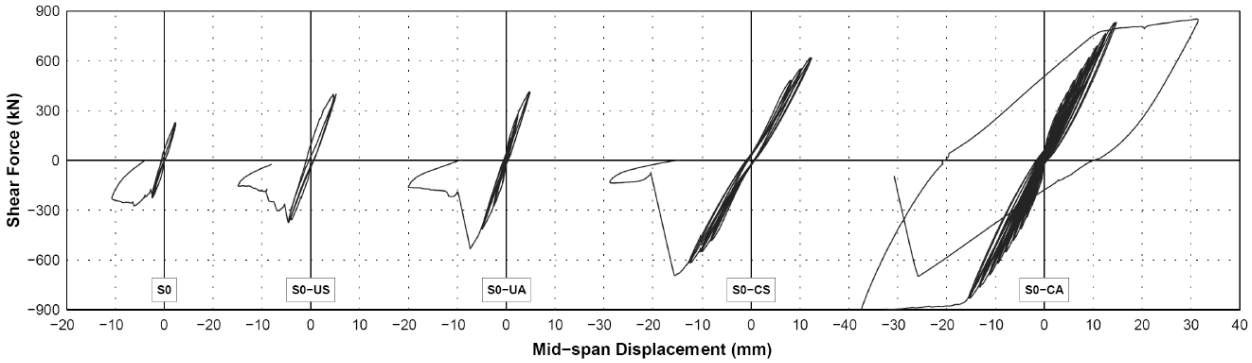

Figure 4. S0 series load-deflection response.

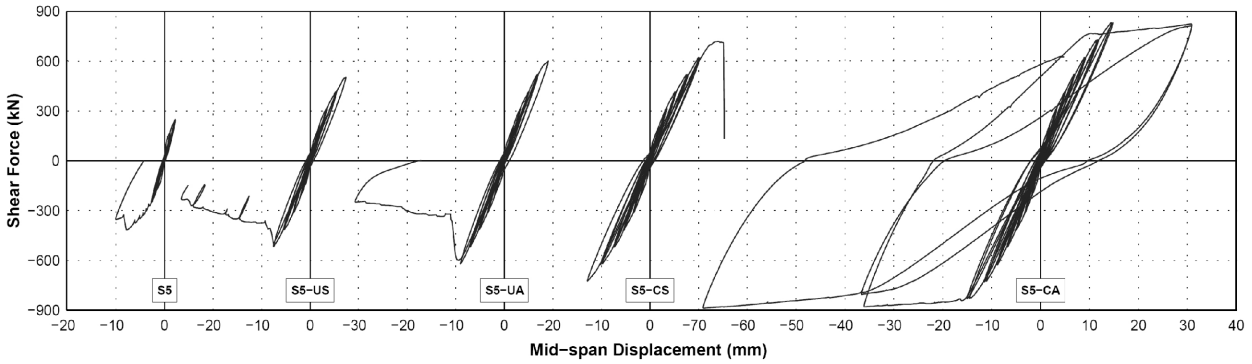

Figure 5. S5 series load-deflection response.

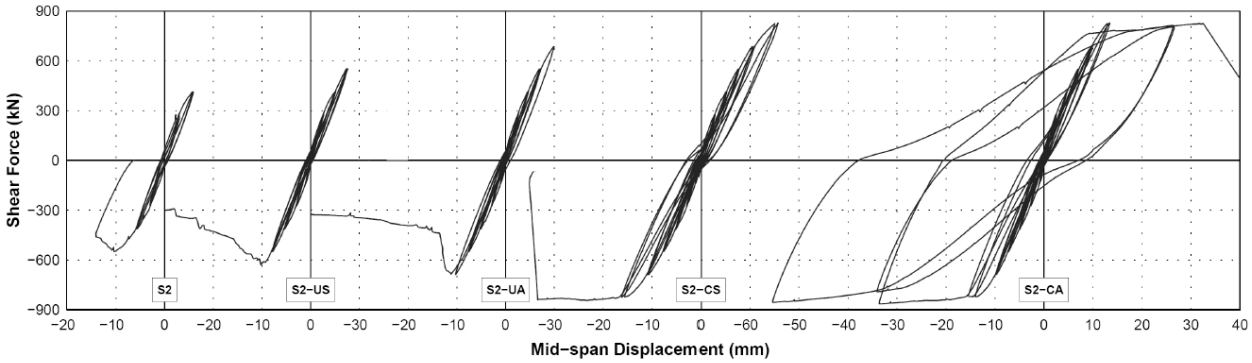

Figure 6. S2 series load-deflection response.

The U-wrapped specimens failed due to debonding, caused by failure within the surface layer of concrete, as opposed to bond failure between the FRP and concrete interface. This was apparent as a fine layer of concrete remained attached to the debonded sheets. In contrast, specimens with closed wraps experienced FRP rupture failure at significantly higher load levels. As shown in Table 1, the maximum shear strength gain was 37% for U-wrapped strips and 94% for U-wrapped sheets, more than 2.5 times the increase for double the amount of FRP. This increase dropped to 2 times and 1.8 times for the S5 and S2 series respectively, as the amount of transverse steel increased. A similar trend was not observed for closed wraps, which had a maximum shear strength gain of 153% for strips and 234% for continuous sheets, an increase of about 1.5 times for double the amount of FRP. This discrepancy may be due to flexural yielding

of the beam prior to FRP rupture for the CA specimens. Flexural yielding occurred at a shear of about 825 kN and mid-span displacements between 12 and 15 mm. With further loading, the FRP ruptured at mid-span displacements over 4 times the yield, indicating a significant reserve of FRP shear capacity.

Table 1. Summary of experimental results.

Specimen	Shear strength, kN	Strength gain from control (%)	Strength gain due to trans. steel (%)	Failure displ. (mm)	Failure mode
S0	275	-	-	6.0	Shear
S0-US	377	37	-	4.6	Shear, FRP debonding
S0-UA	534	94	-	7.4	Shear, FRP debonding
S0-CS	695	153	-	15.5	Shear, FRP rupture
S0-CA	915*	234	-	37.0	Flexure, FRP rupture
S5	415	-	51	7.7	Shear
S5-US	518	25	37	7.6	Shear, FRP debonding
S5-UA	622	50	16	9.1	Shear, FRP debonding
S5-CS	725	75	4	12.6	Shear, FRP rupture
S5-CA	888*	114	-	69.0	Flexure, FRP rupture
S2	551	-	100	10.3	Shear
S2-US	629	14	67	10.2	Shear, FRP debonding
S2-UA	688	25	29	10.3	Shear, FRP debonding
S2-CS	844*	53	21	23.4	Flexure, FRP rupture
S2-CA	866*	57	-	55.3	Flexure, FRP rupture

* indicates maximum shear strength attained after flexural yielding

It is apparent from Table 1, that the gain in shear strength due to the FRP is influenced by the presence of internal transverse steel. Bousselham (2006) concluded that increasing the transverse steel ratio lowers the FRP contribution to shear resistance. For example, the use of U-wrapped strips increased the shear strength of the S0 specimen by 37% from the control, compared with only 25% and 14% increases for the S5 and S2 specimens, respectively. Similarly, the strength gain due to the transverse steel is affected by the FRP. For example, the S5 and S2 controls experience increases in strength of 51% and 100% over the S0 control, which respectively dropped to 37% and 67% due to the application of U-wrapped strips. In general, the strength gain due to transverse steel for S2 was about double that of S5 over the range of specimens that failed in shear, regardless of FRP retrofitting.

Transverse Strains

All S5 and S2 specimens experienced stirrup yielding, as at least one strain gauge at each instrumented section measured strains in excess of the yield. Thus, in accordance with the design codes, the assumption of steel yielding for the determination of ultimate steel shear resistance appears appropriate when FRP is applied. The largest measured FRP strains at debonding failure for the U-wrapped specimens ranged between 0.003 and 0.004, larger than necessary for yielding of the transverse steel. For the closed wrapped specimens, FRP strains in excess of 0.006 were measured. This is significant, as both ACI 440.2R-08 and CSA S6-06 limit the effective strain in

closed wraps to 0.004, attributed with the loss of aggregate interlock in concrete. However, the strain results show that this limit is overly conservative, as it is probable that strains were even higher than those measured with the gauges. Fig. 7 provides an example of the increase in FRP strain with applied load for the S0 and S5 specimens having U-wrapped and closed wrapped sheets. For S0-CA, the FRP strains returned close to zero when the applied load reached zero, but are offset due to concrete cracks not fully reclosing upon load reversals. For S5-CA, a more significant strain offset is apparent at zero load once transverse steel yielding occurred. Plastic deformation beyond stirrup yielding did not permit the FRP strain to release as the load decreased, leaving the FRP permanently strained.

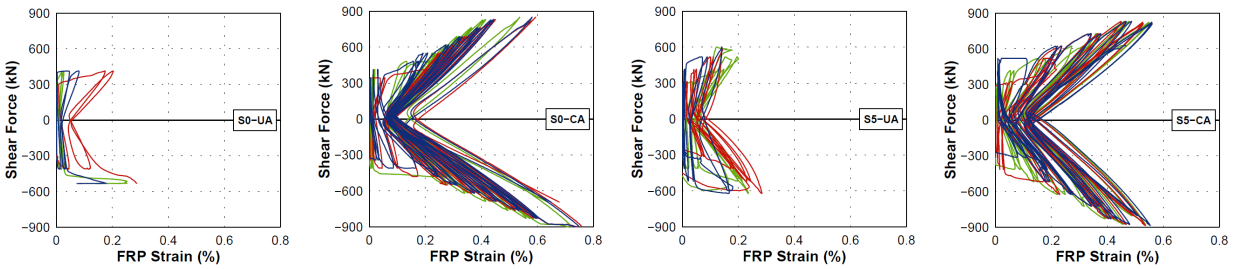

Figure 7. FRP strains curves.

Failure Condition and Crack Pattern

Some S0 series specimens at failure are shown in Fig. 8. The FRP has been removed from those retrofitted with sheets to reveal the cracks beneath. Specimens from the S0 and S5 series, with less than the minimum amount of transverse steel, had single diagonal shear cracks form at their quarter-spans. Having more than minimum transverse steel, the S2 control had several significant shear cracks form, with inclinations less steep than those of S0 and S5, similar to the observations of other researchers (Pellegrino 2002). The presence of FRP is similar to providing more than the minimum amount of transverse reinforcement, as the formation of multiple shear cracks was observed for all retrofitted specimens. The crack inclinations were observed to decrease when FRP was added. For example, within the S0 series the shear crack angle was about 48° for the control and with the addition of FRP the average shear crack angles reduced to between 31° and 36°. For the S5 series, the shear crack angle decreased from 45° for the control to average shear crack angles between 35° and 37° for the retrofitted specimens.

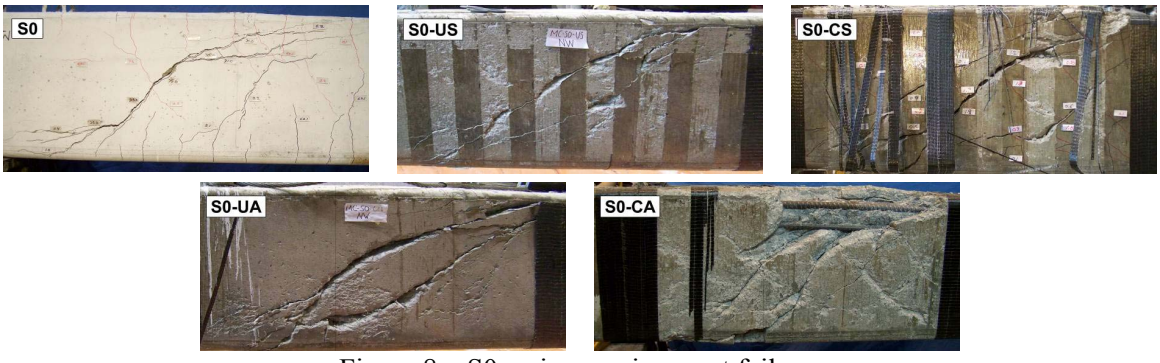

Figure 8. S0 series specimens at failure.

Component Shear Contributions

The shear resistance contributions from the FRP (V_f) and transverse steel (V_s) can be determine from experimental results by two methods, from which the concrete shear resistance (V_c) can then be estimated from the assumption that $V_c = V_{total} - (V_s + V_f)$. The FRP contribution can be obtained by subtraction of the shear capacity of the retrofitted specimens and the control for a particular series, as was done to obtain the strength gains provided in Table 1. In a similar manner, the steel shear capacity can be estimated by comparing specimens in which transverse steel reinforcement is the only variable. The drawback to this method, is that the component contributions are assumed fixed, which may not be reflective of the changes that occur due to the presence of steel or FRP. The second method is to obtain steel and FRP shear contributions from CSA S6-06 formulations, in which the steel yield stress and FRP effective strain are replaced by the average strain gauge measurements at the section with the highest measured strains. From this method, the concrete shear resistance can be estimated with increasing applied shear, as shown in Fig. 9 for several specimens of the S0 and S5 series. Note that these show an envelope of values from downward loading only and that the shear contributions determined in this manner are highly dependent on the shear crack inclination (θ) used, which was difficult to infer due to the presence of multiple crack inclinations. Thus, Fig. 9 shows the trend in shear component resistances calculated assuming the bounds of $\theta = 35°$ and $\theta = 45°$.

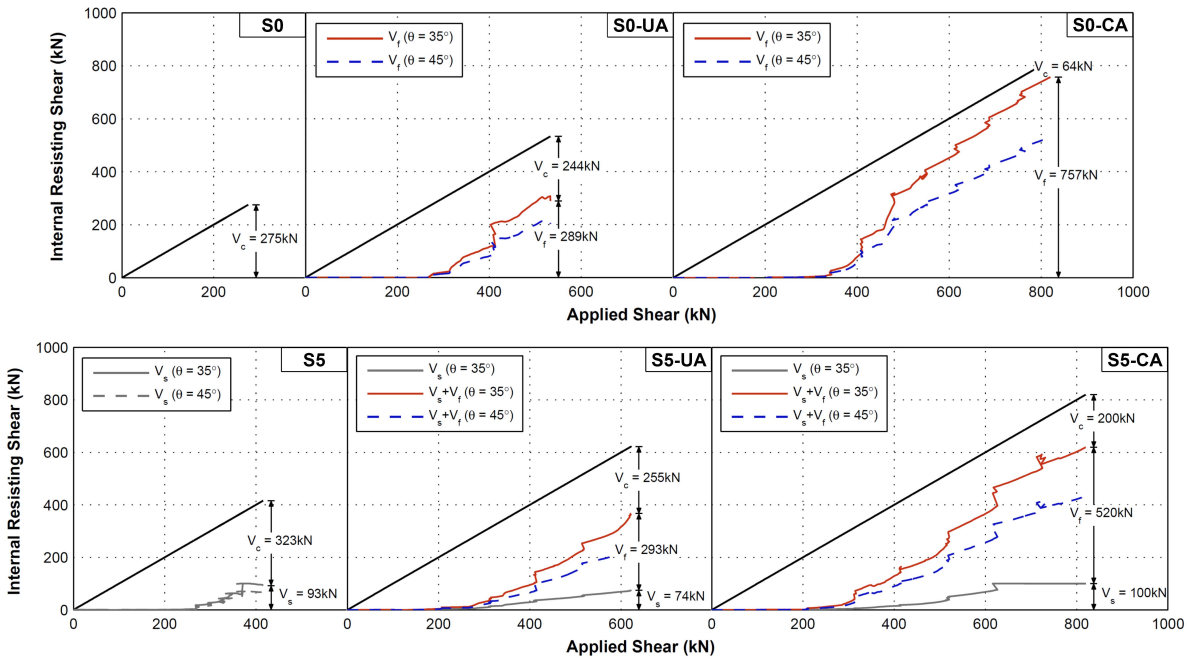

Figure 9. Component shear resistances.

Examination of the S0 series reveals that once FRP activates its shear resistance begins to increase at roughly the same rate as the total shear, despite load reversals as indicated by the jagged parts of the curves. Examination of the S5 series reveals that the transverse steel and FRP activate at about the same load, both increasing at the same rate as the total shear until the steel yields. For S5 control, shear failure occurs shortly after steel yields as the concrete cannot take the burden of further load increase, since the steel contribution remains constant. For the

retrofitted S5 specimens, the FPR continues to strain and resist further increases in load. Thus, the concrete contributions are relatively constant, particularly prior to the occurrence of longitudinal steel yielding at shear force of over 800 kN. Assuming crack inclination values closer to observed averages, it appears that the concrete contribution remains relatively constant with increased load after transverse steel or FRP activate. This implies that the concrete shear contribution can be relied upon under cyclic loading when FRP retrofits are used, as the shear resistance values are close to those of the controls, particularly prior to longitudinal steel yielding. For example, S0 had a shear capacity of 275 kN, whereas after significant load reversals S0-CS had an estimated concrete capacity of 322 kN if the observed crack inclination was used.

FRP Shear Predictions

Provided in Table 2 are the estimated FRP shear contributions as derived from measured strain ($V_{strains}$), and from subtraction between retrofitted and control capacities ($V_{retrofit} - V_{control}$). Since the capacity from strain values changes with the shear crack inclination, the limits of $\theta = 35°$ and $\theta = 45°$ were used to emphases its influence. These estimates are compared with predicted FRP capacities calculated using design codes ACI 440.2R-08, CSA S6-06, and the Italian standard CNR-DT-200/2004. For consistency, the effective FRP depth was assumed equal to $0.9d = 491$ mm for all cases. The effect of varying the crack angle is apparent for a particular specimen, as the predicted FRP shear capacity increases with reduction in the crack inclination. Since ACI 440.2R-08 neglects a variable crack angle, its results are similar to CSA S6-06 with $\theta = 45°$. The CSA S6-06 predictions are relatively close between US and CS specimens, which is contrary to experimental results showing show that CS specimens have over three times the FRP shear capacity of US specimens. This is mainly due to the design code imposed strain limit of 0.004 for closed wraps, resulting in severely underestimated predictions. The CNR-DT-200/2004 predictions are closest to experimentally derived FRP shear capacities, although the accuracy is dependent on the assumed crack angle. Overall, the reduction in FRP capacity due to the presence of transverse steel remains unaccounted-for in any of the current design codes.

Table 2. Predicted and estimated FRP shear capacities.

	FRP retrofit type:	U-wrap strips (US)		U-wrap sheet (UA)		Closed strips (CS)		Closed sheets (CA)	
	Assumed crack angle (θ):	45°	35°	45°	35°	45°	35°	45°	35°
Predicted	V_f predicted (kN)								
	ACI 440.2R-08	161	-	323	-	185	-	370	
	CSA S6-06	161	230	323	461	185	264	370	529
	CNR-DT-200/2004	97	139	186	266	305	435	583	832
Experimental	$V_{strains}$ (kN)								
	S0 series	82	118	203	289	291	415	530	757
	S5 series	131	188	205	293	273	390	364	520
	S2 series	125	178	206	295	255	364	287	410
	$V_{retrofit} - V_{control}$ (kN)								
	S0 series	102		259		420		640	
	S5 series	103		207		310		473	
	S2 series	78		137		293		315	

Concluding Remarks

Carbon FRP was found to be extremely effective at improving the shear performance of relatively large shear-critical reinforced concrete beams under simulated seismic load. The presence of internal transverse steel affected the crack pattern and diagonal crack inclination, in addition to reducing the FRP shear strength gain. The maximum measured FRP strains for closed wraps were significantly larger than the design code limit of 0.004, which when used resulted in underestimated shear strengths. The concrete shear resistances remained relatively constant throughout reversed cyclic loading and were close to design code predicted concrete shear strengths. No significant reduction in FRP performance was observed due to cycling, particularly when compared with code predictions, which inaccurately estimate the FRP potential regardless of loading type. Thus, it is believed that the FRP is capable of acting in a seismic event to improve shear capacity and maintain the concrete shear contribution.

Acknowledgments

Funding for this research was provided by the Natural Sciences and Engineering Research Council of Canada (NSERC) and ISIS Canada, a NSERC Network of Centres of Excellence.

References

American Concrete Institute, 2008. *Building Code Requirements for Structural Concrete and Commentary* (ACI 318-08), Farmington Hills, Michigan.

American Concrete Institute, 2008. *Guide for Design and Construction of Externally Bonded FRP Systems for Strengthening Concrete Structures* (ACI 440.2R-08), Farmington Hills, Michigan.

Anil, O., 2006. Improving Shear Capacity of RC T-beams Using CFRP Composites Subjected to Cyclic Loading, *Cement & Concrete Composites* 28 (7), 638-649.

Bousselham, A. and Chaallal, O., 2006. Effect of Transverse Steel and Shear Span on the Performance of RC Beams Strengthened in Shear with CFRP, *Composites: Part B* 37 (1), 37-46.

Canadian Standards Association, 2004. *Design of Concrete Structures* (CAN/CSA A23.3-04), Mississauga, Ontario.

Canadian Standards Association, 2006. *Canadian Highway Bridge Design Code* (CAN/CSA S6-06), Mississauga, Ontario.

Consiglio Nazionale delle Ricerche, 2004. *Guide for Design and Construction of Externally Bonded FRP Systems for Strengthening Existing Structures* (CNR-DT-200/2004), Rome, Italy.

Duong, K.V., Sheikh, S.A. and Vecchio, F.J., 2007. Seismic Behaviour of Shear-Critical Reinforced Concrete Frame: Experimental Investigation, *ACI Structural Journal* 104 (3), 304-313.

Pellegrino, C. and Modena, C., 2002. Fibre Reinforced Polymer Shear Strengthening of Reinforced Concrete Beams with Transverse Steel Reinforcement, *J. Composites for Construction* 6 (2), 104-111.

Sakar, G. Tanarslan, H.M., and Alku, O.Z., 2009. An Experimental Study on Shear Strengthening of RC T-section Beams with CFRP Plates Subject to Cyclic Load, *Mag. of Concrete Research* 61 (1), 43-45.